# Low-Dose FK-506 Contributes to Tubulointerstitial Fibrosis Through Epithelial-Stromal Interactions

FK-506 en Dosis Bajas Contribuye a la Fibrosis Túbulointersticial Mediante Interacciones Epiteliales-Estromales

Youngmin Yoon<sup>1</sup>; Hyun Lee Kim<sup>1</sup>; Byung Chul Shin<sup>1</sup> & Sang-Pil Yoon<sup>2</sup>

YOON, Y.; KIM, H. L.; SHIN, B. C. & YOON, S. P. Low-dose FK-506 contributes to tubulointerstitial fibrosis through epithelial-stromal interactions. *Int. J. Morphol.*, 43(5):1662-1673, 2025.

SUMMARY: FK-506 is a widely used immunosuppressive drug for renal transplantation, but has a common side effect of progressive tubulointerstitial fibrosis. Although fibroblasts have been receiving attention for the fibrogenesis, the roles of renal epithelial cells are remained to be further investigated. Therefore, we aimed to assess the responses of renal epithelial cells compared to the renal interstitial fibroblasts after FK-506 treatment for fibrogenesis. We adopted renal proximal tubule cells (NRK-52E) and interstitial fibroblast cells (NRK-49F) isolated from rats for the FK-506-induced renal fibrogenesis. The responses after FK-506 treatment were assessed by cell viability assay, spheroidogenesis, Western blotting, and immunocytochemistry. NRK-52E cells showed higher N-cadherin while NRK-49F cells showed higher E-cadherin, fibronectin, and alpha-smooth muscle actin (αSMA). As compared to NRK-52E cells, NRK-49F cells showed higher sensitivity to FK-506 by cell viability and spheroidogenesis. Spheroidogenesis was induced by the increased fibronectin and vimentin in both cells, while cell adhesion molecules as well as αSMA were decreased. The more sensitive NRK-49F cells showed a trend of increase in apoptosis after FK-506 treatment, but autophagy, ferroptosis, and cell cycle did not affect both cell lines. Low-dose FK-506 transiently increased αSMA expression in NRK-52E cells, which was also confirmed by co-cultured NRK-52E cells as accompanied by fibronectin. Taken together, NRK-52E cells showed fibrogenic responses following low-dose FK-506 treatment with an increased αSMA and fibronectin expression, which was disappeared after high-dose FK-506 treatment. As fibrogenesis markers were differentially expressed in various renal cell lines, further research through more detailed experimental design should be performed.

KEY WORDS: FK-506; Fibrosis; Proximal tubule cell; Marker.

### INTRODUCTION

Calcineurin inhibitor (cyclosporine A and FK-506 (tacrolimus))-induced chronic nephropathy can occur independently of acute renal dysfunction, dosage or blood concentration and shows progressive tubulointerstitial fibrosis (Olyaei *et al.*, 1999). In spite of the therapeutic benefits of calcineurin inhibitors, renal fibrosis still represents a common side effect of long-term therapy (Eberhardt *et al.*, 2018). The calcineurin inhibitor-induced increase in transforming growth factor-beta (TGF- $\beta$ ) and subsequent activation of signaling pathways, especially on Smad3 (Sakairi *et al.*, 2011; Baba *et al.*, 2015; Sasaki *et al.*, 2016; Chen *et al.*, 2018; Zhou *et al.*, 2021a), is known to be closely associated with the chronic nephropathy.

FK-506-induced chronic nephrotoxicity animal model is well-established in rats (Zheng *et al.*, 2021; Nady *et al.*,

2024) and mice (Cao et al., 2023), which is comparable to tubulointerstitial fibrosis with an increased alpha-smooth muscle actin (aSMA) and/or fibronectin. While apoptosis is increased simultaneously, autophagy is reported as increased (Zheng et al., 2021) or decreased (Cao et al., 2023) in HK-2 human proximal tubule cells. FK-506 causes a fibrogenic response (Deng et al., 2016) through profibrogenic TGF-β activation, results in an increased aSMA as a fibroblast activation marker (Shigematsu et al., 2022) in both renal epithelial cells (NRK-52E) and renal interstitial fibroblasts (NRK-49F) isolated from rats. Although αSMA is widely used marker for TGF-β-induced fibrosis (Chang et al., 2012; Liang et al., 2021; Zhou et al., 2021a; Huang et al., 2022; Hira et al., 2022, Wang et al., 2024b), fibronectin and vimentin are also adopted (Chang et al., 2012; Liang et al., 2021; Wang et al., 2024b) in renal tubulointerstitial fibrosis research.

Received: 2025-06-18 Accepted: 2025-07-24

<sup>&</sup>lt;sup>1</sup> Division of Nephrology, Department of Internal Medicine, Chosun University Hospital, Chosun University College of Medicine, Gwangju, Republic of Korea.

<sup>&</sup>lt;sup>2</sup>Department of Anatomy, College of Medicine, Jeju National University, Jeju, Republic of Korea.

FUNDING. This study was supported by the 2025 scientific promotion program funded by Jeju National University.

More attention has been paid to the responses of fibroblasts as compared to the tubular epithelial cells. Cisplatin induces renal interstitial fibrosis with increased αSMA in myofibroblast transformed NRK-49F cells, not in NRK-52E cells (Yano et al., 2015). While cisplatininduced premature senescence was observed in NRK-52E and NRK-49F cells (Zheng et al., 2023), repeated low dose cisplatin induced fibroblast-to-myofibroblast transformation more effectively than high dose cisplatin in NRK-49F cells (Yu et al., 2022, 2024). When co-cultured with NRK-49F and RAW264.7 cells, tubulointerstitial fibrosis was augmented through epithelial-mesenchymal transition (EMT) and macrophage-myofibroblast transition through increased aSMA and fibronectin and decreased E-cadherin (Cao et al., 2022). When co-cultured with NRK-52E cells (Schulz et al., 2019; Liang et al., 2021; Wang et al., 2024b) or purified exosome from hypoxic NRK-52E cells (Zhou et al., 2021b) or TGFβ-stimulated NRK-52E cells (Zhao et al., 2021), NRK-49F cells are activated, secrete fibronectin, aSMA, or collagen I, and then aggravate renal fibrosis. When co-cultured, NRK-52E cells also activate NRK-49F cells through increased fibronectin and vimentin (Schulz et al., 2019) or decreased peroxisome proliferator-activated receptor alpha (Wang et al., 2024a). In addition, NRK-49F cells when co-cultured with mouse proximal tubule cells (BUMPT) showed increased expression of fibronectin, aSMA, and type I collagen (Wen et al., 2020).

We focused on the previous findings that tubular epithelial cell vacuolation, atrophy and microcalcification may be associated with the development of irreversible interstitial fibrosis under FK-506 treatment (Finn, 1999). Fibrogenesis characterized by an increased fibronectin as well as type I collagen was not associated with an increase in hyperplasia either in tubuloepithelial cells or in interstitial fibroblasts (Ruiz-Ortega *et al.*, 1998). Likewise, increased fibronectin and  $\alpha$ SMA and decreased E-cadherin in NRK-52E cells were observed under cyclosporine A-induced fibrosis (Ardura *et al.*, 2008). Fibrogenesis was also confirmed by an increased fibronectin in both NRK-52E and NRK-49F cells, but  $\alpha$ SMA only in NRK-52E cells (Yang *et al.*, 2010).

To clarify the cell type-dependent responses, respective markers for renal epithelial cells and renal interstitial fibroblasts have been used. Recently, E-cadherin is used for renal proximal tubule (Ardura *et al.*, 2008; Chen *et al.*, 2018; Schulz *et al.*, 2019, 2022; Liang *et al.*, 2021; Cao *et al.*, 2022; Sun *et al.*, 2025) and N-cadherin for fibroblasts (Schulz *et al.*, 2019) in quantitative studies. However, N-cadherin is the predominant cadherin in the renal proximal tubule while E-cadherin is abundant in other

nephron segments (Prozialeck *et al.*, 2003, 2004; Nürnberger *et al.*, 2010; Keller *et al.*, 2012) in qualitative studies. We noted that this discrepancy on specific markers might be ignored without receiving particular interest.

Therefore, we aimed to investigate the respective fibrogenic responses following FK-506 treatment, focusing on the renal epithelial cells and interstitial fibroblasts. The specific markers for renal epithelial cells and interstitial fibroblasts, for fibrogenesis, and for programmed cell deaths were adopted to assess the respective responses following FK-506 treatment in a dose-dependent manner.

#### MATERIAL AND METHOD

Cell lines and culture. Normal kidney proximal tubule cell line from human (HK-2), pig (LLC-PK1), rat (NRK-52E), mouse (TCMK1), and cat (CRFK) and normal rat kidney fibroblast cell line (NRK-49F) were kindly provided by Professor Jinu Kim (Jeju National University, Jeju, Republic of Korea). HK-2 cell line was cultured in RPMI 1640 medium and others in Dulbecco's Modified Eagle Medium (DMEM) enriched with 10 % fetal bovine serum, 100 unit/mL penicillin, and 0.1 mg/mL streptomycin at 37 °C in a 5 % CO<sub>2</sub> atmosphere. All cell culture reagents were purchased from Corning Inc. (Corning, NY, USA).

Co-culture with NRK-52E and NRK-49F. The indirect co-culture method was used with a slight modification to induce injury and fibrotic phenotype of renal tubular cells as previously reported (Schulz et al., 2023), which suggested the longest possible incubation time (48 h) without critical decreased in cell viability. NRK-49F cells were grown on permeable filter inserts (pore size 0.4 μm) and NRK-52E cells were grown in 24-transwell plates for cell viability assay or 6-transwell plates for western blotting. In the transwell condition, there was no direct contact between cells due to the pore size and the transwell membrane. NRK-52E, NRK-49F, and the co-cultured cells were treated with or without FK-506 at a concentration of 10 µM for 48 h and then 30 µM for 48 h. Thereafter, the cells were processed separately and used for the following experiments.

Cell viability assay. NRK-52E and NRK-49F cells were seeded in triplicate wells of 96-well plates and tracked the proliferation rate up to 48 h. Cells were treated with FK-506 (0, 0.1, 1, 10, 30, and 100  $\mu$ M) and incubated for 48 h for cell viability assay. The cells in transwell co-culture environment were treated with FK-506 (0 and 10  $\mu$ M) for 48 h, and then further treated with FK-506 (0 and 30  $\mu$ M) with new culture medium for 48 h.

MTT (ThermoFisher Scientific, Waltham, MA, USA; #M6494) was utilized to assess cell viability following established protocols (Yoon, 2024). Absorbance measurements were obtained at 595 nm, with a reference wavelength of 620 nm, using a VERSAmax microplate reader (Molecular Devices Korea LLC.; Seoul, Republic of Korea). Cell viability percentages were calculated based on the average absorbance of triplicate wells, with the 50 % cytotoxicity concentration (IC $_{50}$ ) calculated by MS Excel 2016.

**Spheroid culture.** Ultra-low attachment 96-well plates were purchased from Corning Inc. to create an anchorage-independent environment. NRK-52E and NRK-49F cells were cultured with 1 % B27 supplement (#17504-044), 20 ng/ml epidermal GF (#PHG0311) and 20 ng/ml basic fibroblast GF (#13256029; all from Thermo Fisher Scientific) in DMEM/F12 medium (Corning Inc.) as previously reported (Chang *et al.*, 2021; Chang & Yoon, 2023).

The cells were treated with FK-506 (0, 0.1, 1, 10, and 30  $\mu$ M), and the spheroidogenic capacity was calculated by multiplying the number by the size of spheroids on day 7 in flat-bottom plates. The spheroids were collected using a cell strainer with a pore size of 70  $\mu$ m (Corning Inc., #CLS431751), washed with ice-cold PBS, and then prepared for Western blotting.

The respective spheroidogenesis was checked by morphometry on day 5 and up to day 15 in round-bottom plates. To compare the spheroidogenic capacity, different seeding condition was adopted as NRK-52E (200 cells/well), NRK-49F (200 cells/well), and NRK-52E (100 cells/well) co-seeded with a serial dilution of NRK-49F cell (100 to 3 cells/well).

Western blotting. Electrophoresis of the total protein in cell lysis buffer was executed utilizing 12 % or 7.5 % polyacrylamide gels in conjunction with the TGX FastCast acrylamide kit (Bio-Rad Laboratories, Hercules, CA, USA; #1610175 or #1610171) and a designated running buffer (Bio-Rad Laboratories, # TR2015-100-00), followed by transfer onto a polyvinylidene fluoride membrane (Bio-Rad Laboratories, #162-0176) using a specific transfer buffer (Bio-Rad Laboratories, #TR2028-100-00), as described previously (Chang *et al.*, 2021; Chang & Yoon, 2023; Yoon, 2024).

The membrane was subjected to incubation at 4 °C for 18 h with various antibody-targeting proteins, including αSMA (Sigma-Aldrich, St. Louis, MO, USA; #A5228), vimentin (Santa Cruz Biotechnology, Santa Cruz, CA,

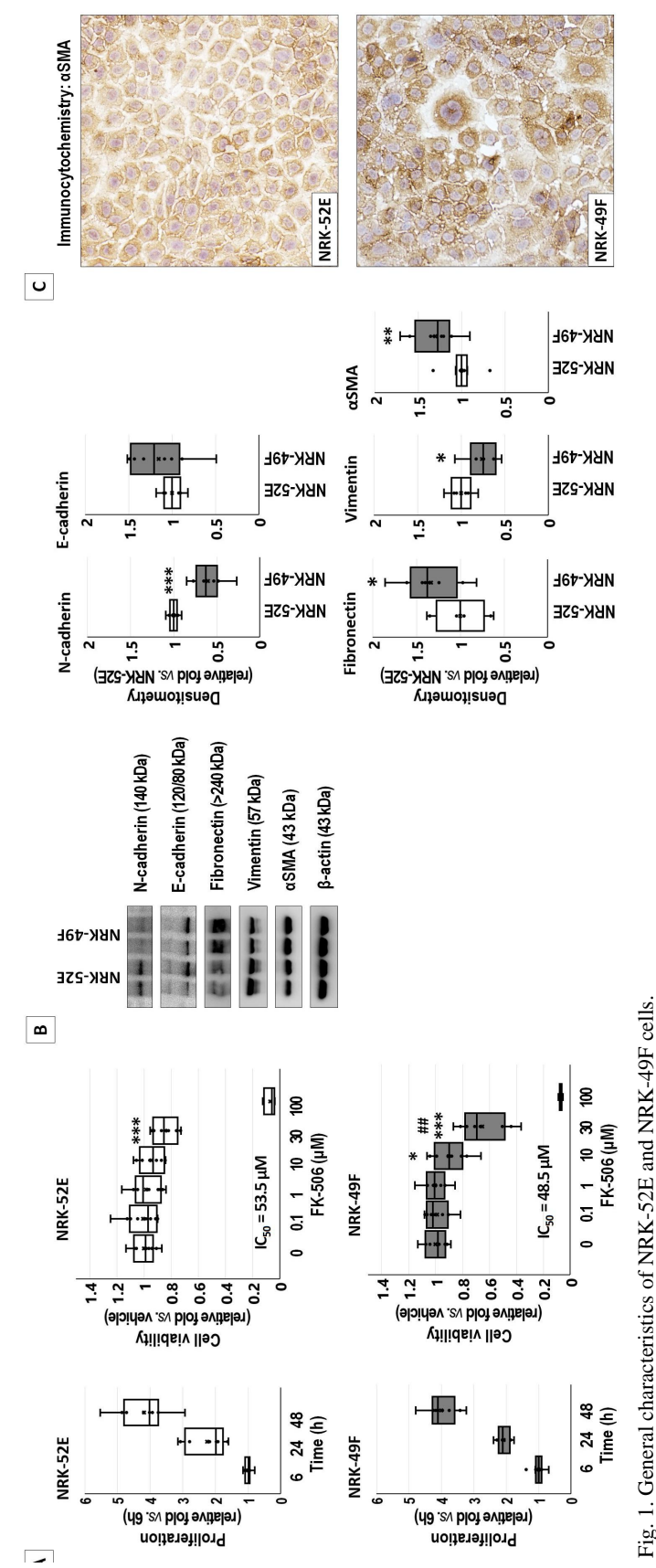
USA; #sc-6260), fibronectin (ABclonal, Woburn, MA, USA; #A12932), N-cadherin (Cell Signaling Technology, Beverly, MA, USA; #4061), E-cadherin (Santa Cruz Biotechnology, #sc-7870), PARP1 (Cell Signaling Technology, #9542), LC3 (Cell Signaling Technology, #12741), GPX4 (Santa Cruz Biotechnology, #sc-166570), P27 (Cell Signaling Technology, #2552), and b-actin (Santa Cruz Biotechnology; #sc-47778). Subsequently, peroxidase-conjugated anti-rabbit (Vector Laboratories, Burlingame, CA, USA; #WB-1000) and peroxidase antimouse (Vector Laboratories; #WB-2000) IgG antibodies were applied for 1 h at room temperature. Protein expression was subsequently visualized through the Azure c300 imaging system (Azure Biosystems, Dublin, CA, USA). Quantification of protein levels was performed employing the AzureSpot analysis software (version 14.2; Azure Biosystems).

Immunocytochemistry. Immunocytochemistry was conducted on a 12 mm cover glass in 12-well plates, following established protocols (Yu *et al.*, 2024). Cells underwent fixation with ice-cold methanol, blocked with 10 % normal horse serum for 1 h, and were subsequently stained with aSMA antibody for overnight at 4 °C. Antimouse (1:200 dilution; Vector Laboratories; #PI-2000) IgG antibody was applied before counterstaining the nuclei with Hematoxylin (#H3404, Vector Laboratories) for 1 min. Immunolabelled images were directly captured using a DP22 digital camera and BX-51 light microscope (Olympus, Tokyo, Japan).

**Statistics.** Statistical analysis of the data was conducted using MS Excel 2016. Data are expressed as the mean values  $\pm$  SD from a minimum of three replicate experiments if not specified. Statistical significance was determined by t-test between 2 groups or one-way analysis of variance (ANOVA) over 3 groups followed by a *post-hoc* test. A value of p < 0.05 was considered statistically significant.

#### RESULTS

General characteristics of NRK-52E and NRK-49F cells. Two cell lines showed similar proliferation curves without considerable difference (p=0.326). The IC $_{50}$  value of NRK-52E and NRK-49F cells against FK-506 was 53.5  $\mu$ M and 48.5  $\mu$ M. NRK-49F cells showed a significant decrease in cell viability at 10  $\mu$ M (90.1  $\pm$  12.8 %, p=0.026); while NRK-52E cells (94.3  $\pm$  9.3 %; p=0.084) did not. Intercellular differences were significant at 30  $\mu$ M (p=0.003) in NRK-52E (84.4  $\pm$  8.5 %) and NRK-49F (65.3  $\pm$  16.5 %) cells. Collectively, NRK-49F cells showed more sensitivity against FK-506 treatment than NRK-52E cells (Fig. 1A).

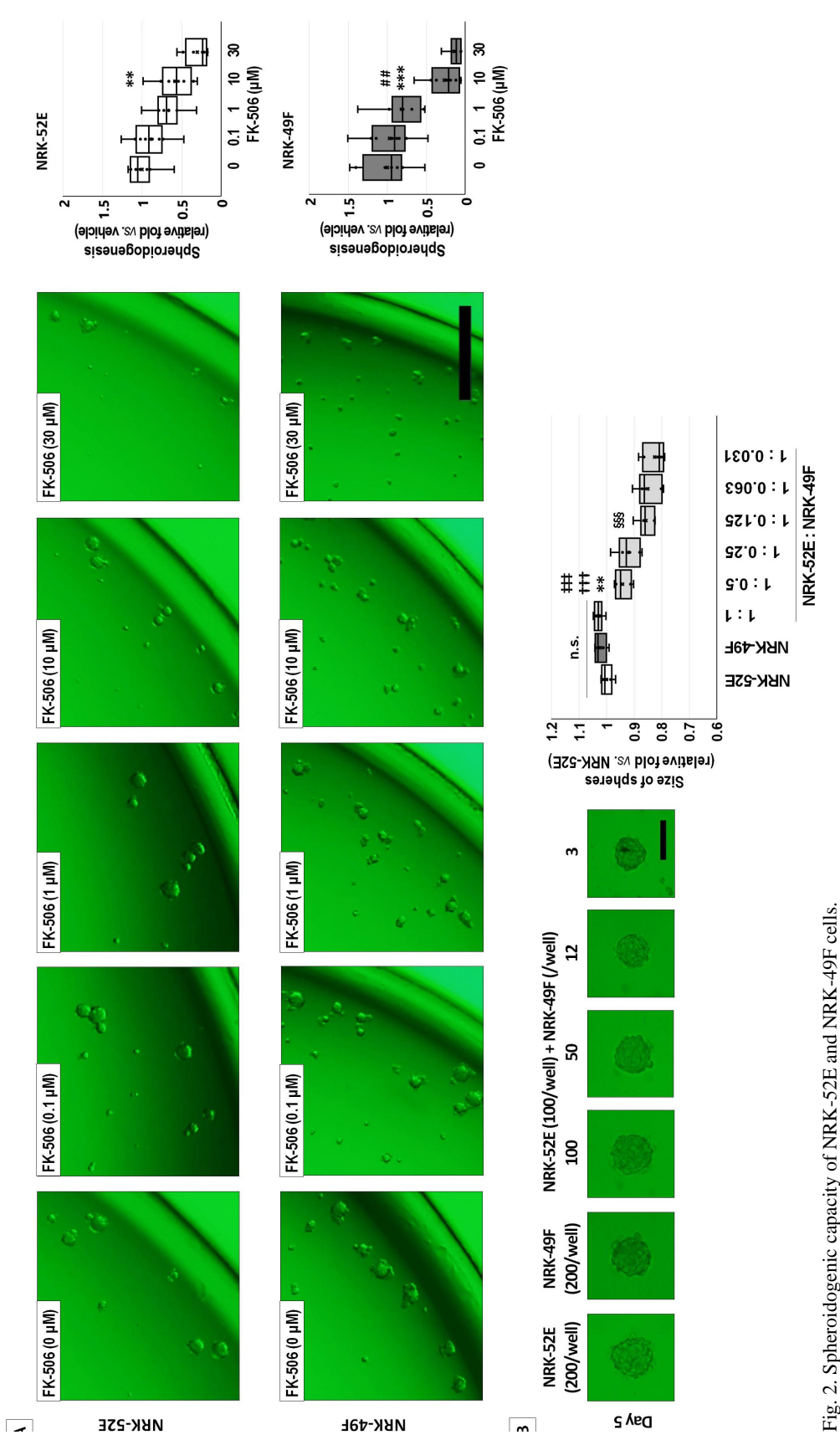


B. Cells were mock-treated with DMSO or treated with indicated dose of FK-506 for 2 days. Cells were harvested and whole cell extracts were subjected to immunoblotting using A. NRK-52 and NRK-49F cells were mock-treated with dimethyl sulfoxide (0) or treated with indicated concentrations of FK-506 for 2 days. The proliferation and extent of cell the indicated antibodies. Signal intensities of N-cadherin, E-cadherin, fibronectin, vimentin, &SMA, and b-actin were measured by AzureSpot analysis software. Each density was viability was determined by MTT assay as described in Methods. Data are presented as mean  $\pm$  SD. \*p<0.05, \*\*\*p<0.001 vs. vehicle; ##p<0.01 vs. NRK-52E. p<0.05, \*\*p<0.01, \*\*p<0.001 vs. vehicle. C. NRK-52 and NRK-49F cells were immunostained with  $\alpha$ SMA antibody as described in Methods. normalized as compared to  $\beta$ -actin, and data are presented as the mean  $\pm$  SD.

To reveal the general characteristics of both cell lines, Western blotting was adopted (Fig. 1B). As compared to NRK-52E cells, NRK-49F cells showed lower expression on N-cadherin (0.60 ± 0.18 fold; p=0.000) and vimentin  $(0.76 \pm 0.18 \text{ fold}; p=0.014)$ , but higher on fibronectin  $(1.34 \pm 0.33)$ fold; p=0.023) and  $\alpha$ SMA (1.30  $\pm$ 0.26 fold; p=0.008). Taken together, NRK-52E cells are compatible for renal proximal tubule cells and NRK-49F cells are renal fibroblasts. The immunocytochemistry with αSMA showed stronger intensity in NRK-49F (Fig. 1C).

Spheroidogenic capacity of NRK-52E and NRK-49F cells. FK-506 affects spheroidogenesis of NRK-52E and NRK-49F cells (Fig. 2A). When treated with FK-506, the number (p<0.001) and the size (p<0.001) of spheres were significantly decreased in a dosedependent manner in both cell lines. The spheroidogenic capacity of NRK-52E cells was decreased at 1  $\mu$ M FK-506 (0.68  $\pm$  0.21 fold, p=0.003) and 10 mM (0.58  $\pm$  0.22 fold, p=0.001). The spheroidogenic capacity of NRK-49F cells was decreased at 10 µM FK-506 (0.27  $\pm$  0.21 fold, p<0.001), which showed a statistical significance between cell lines (p=0.006).

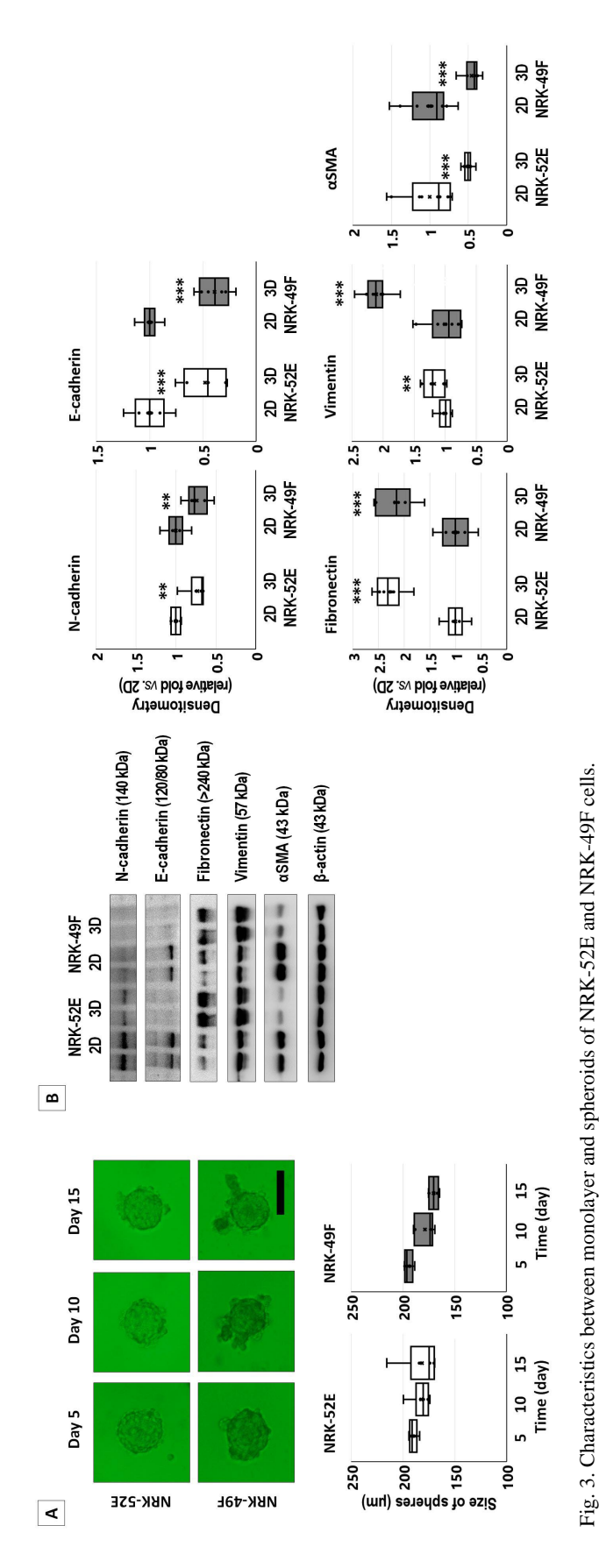
Spheroidogenesis showed the seeding number-dependency, not the cell line (Fig. 2B). The total seeding number was equal; the respective sizes of spheres were compatible among NRK-52E cells, NRK-49F cells, and co-seeding. When co-seeded with NRK-52E and NRK-49F cells, spheres were considerably decreased at 1:0.5 (0.94 ± 0.03 fold, p=0.001 vs. NRK-52E; p=0.000 vs. NRK-49F; p<0.001 vs. 1:1) and 1:0.125 (0.86 ± 0.03 fold, p=0.000 vs. 1:0.5) ratio.



B. NRK-52 and NRK-49F cells were cultured supplemented with growth factors in a round-bottom ultralow attachment well for 5 days, in a number-dependent manner. Size of ultralow attachment well for 7 days. Spheroidogenic capacity was calculated by multiplying the number by the size of spheroids as described in Methods. \*\*p<0.01, \*\*\*p<0.001 vs. vehicle; ##p<0.01 vs. NRK-52E.

A. NRK-52 and NRK-49F cells were mock-treated with dimethyl sulfoxide (0) or treated with indicated concentrations of FK-506 supplemented with growth factors in flat-bottom

spheroids were measured and compared as described in Methods. n.s., not significant; \*\*p<0.01 vs. NRK-52E; ##p<0.01 vs. NRK-49F; †††p<0.001 vs. 1.1; §§§p<0.001 vs. 1:0.5.



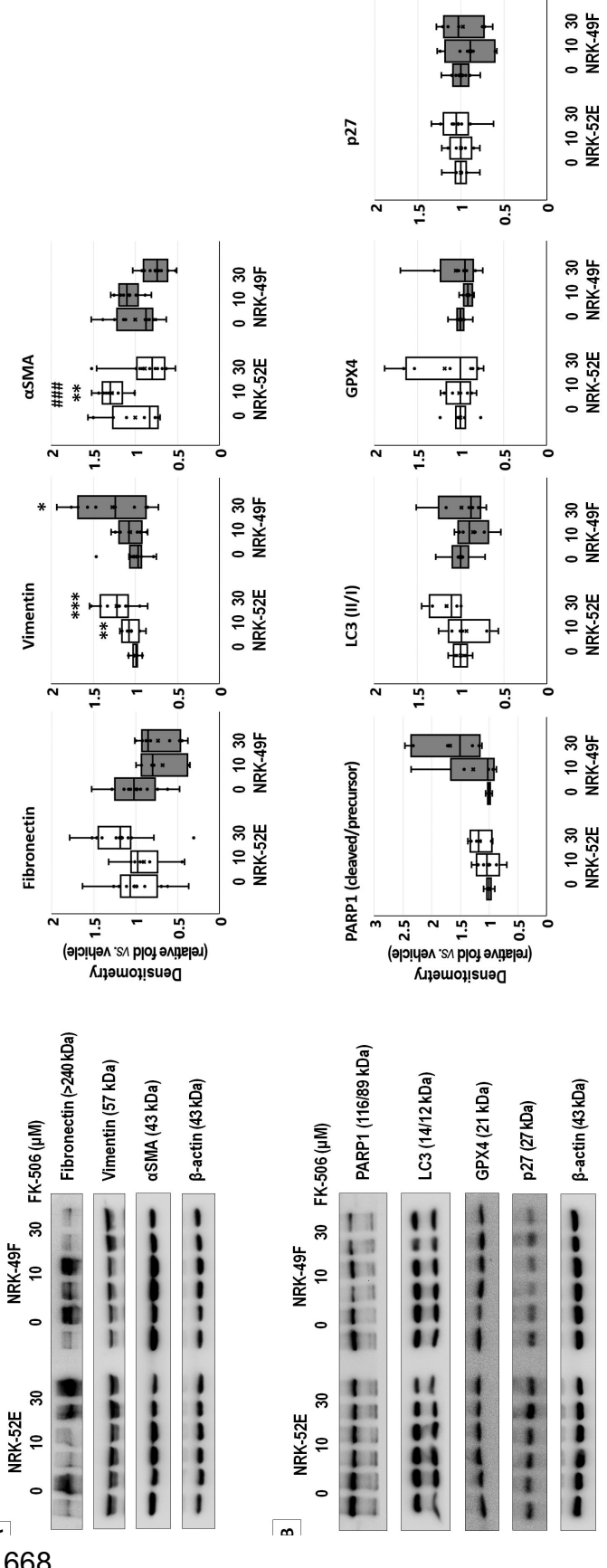
A. NRK-52 and NRK-49F cells were cultured supplemented with growth factors in a round-bottom ultralow attachment well for 15 days. Size of spheroids were measured and B. Cells were cultured in 2-dimensional (2D) or 3-dimensional (3D) environments for 2 days. Cells were harvested and whole cell extracts were subjected to immunoblotting using the indicated antibodies. Signal intensities of N-cadherin, E-cadherin, fibronectin, vimentin, αSMA, and b-actin were measured by AzureSpot analysis software. Each density was normalized as compared to b-actin, and data are presented as the mean  $\pm$  SD. \*p<0.05, \*\*p<0.01, \*\*\*p<0.001 vs. 2D. compared at day 5.

Characteristics between 2D and 3D of NRK-52E and NRK-49F cells. Both cell lines were not proper for long-term culture of spheres (Fig. 3A). The spheres from both cell lines did not grow as time goes by, in which NRK-49Fcells considerably decreased (194.8  $\pm$  4.2 to 170.4  $\pm$  4.7  $\mu$ m; p=0.000).

When compared with 2D conventional culture, respective spheroids from NRK-52E and NRK-49F cells showed lower expression in N-cadherin (0.73  $\pm$  0.13 fold; p=0.001 vs. 0.74  $\pm$  0.14 fold; p=0.004), E-cadherin (0.48  $\pm$  0.19 fold; p=0.000 vs. 0.39  $\pm$  0.15 fold, p<0.001), and aSMA (0.50  $\pm$  0.06 fold, p<0.001 vs. 0.45  $\pm$  0.11 fold, p<0.001), but higher expression in fibronectin (2.29  $\pm$  0.28 fold, p<0.001 vs. 2.17  $\pm$  0.37 fold, p<0.001) and vimentin (1.17  $\pm$  0.16 fold, p=0.007 vs. 2.11  $\pm$  0.21 fold, p<0.001) (Fig. 3B).

Dose-dependent effects of FK-506 in NRK-52E and NRK-49F cells. The changes on fibrosis markers were investigated after FK-506 treatment by Western blotting (Fig. Fibronectin did not show considerable changes in both cell lines. Vimentin expression was significantly increased in a dose-dependent manner in both NRK-52E (p<0.001) and NRK-49F (p=0.039) cells. αSMA showed a dosedependent decrease (p=0.010 and p=0.002), but transiently increased at 10 µM FK-506 treatment in NRK-52E  $(1.28 \pm 0.17 \text{ fold}, p=0.010)$  and NRK- $49F (1.08 \pm 0.15 \text{ fold, p=0.196}) \text{ cells.}$ 

The changes on cell death or cell cycle arrest markers were further examined after FK-506 treatment (Fig. 4B). The activation of PARP1 (cleaved/precursor), LC3 (II/I), GPX4, and p27 did not show any considerable changes in both cell lines, while PARP1 activation showed a dosedependent tendency in NRK-49F (p=0.073).



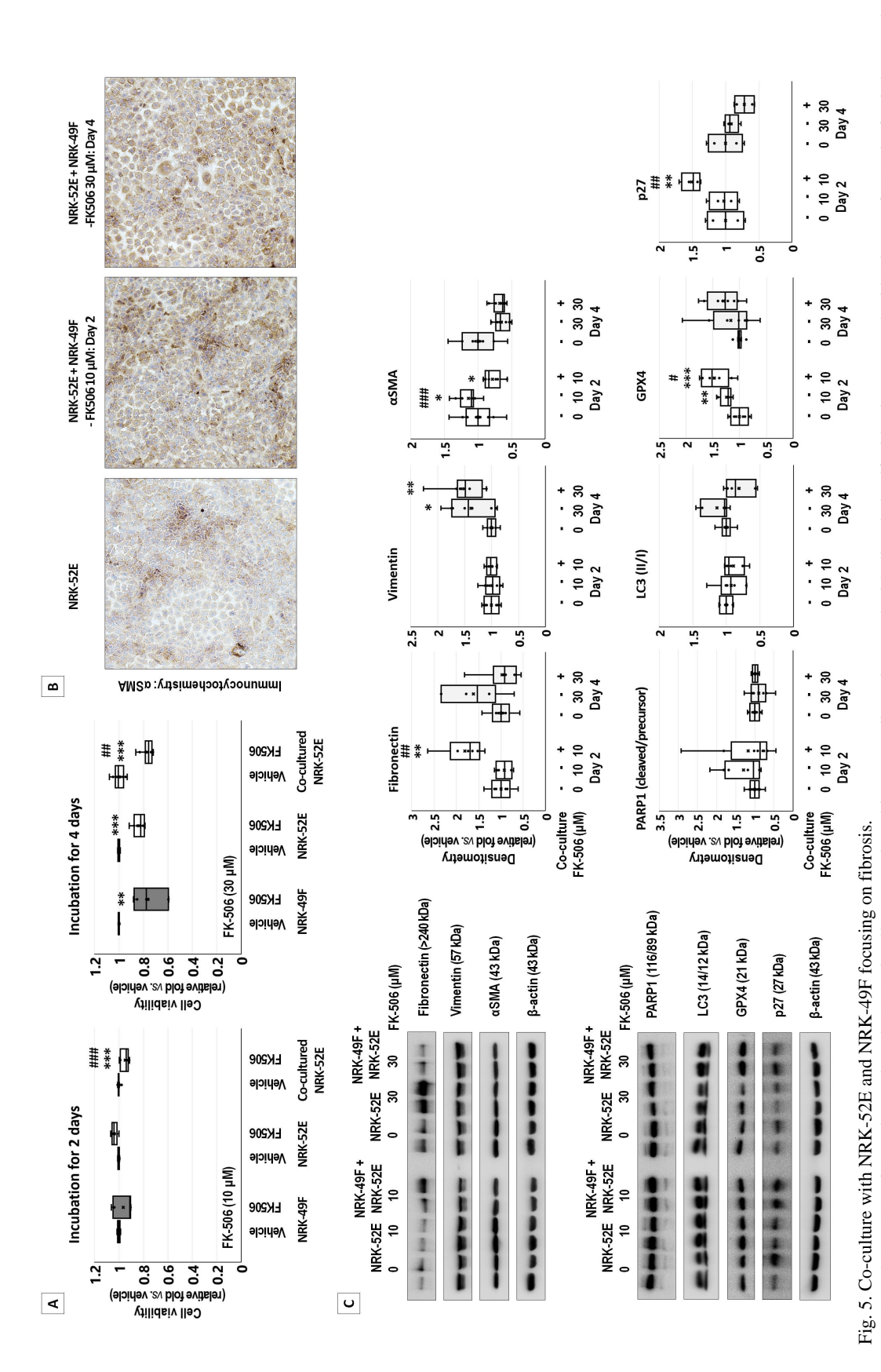
A. Cells were mock-treated with dimethyl sulfoxide (0) or treated with indicated dose of FK-506 for 2 days. Cells were harvested and whole cell extracts were subjected to immunoblotting using the indicated antibodies. Signal intensities of fibronectin, vimentin, αSMA, and b-actin were measured by AzureSpot analysis software. Each density was B. The samples prepared in (A) were subjected to immunoblotting using the indicated antibodies. Signal intensities of PARP1, LC3, GPX4, p27, and b-actin were measured by normalized as compared to b-actin, and data are presented as the mean  $\pm$  SD. \*p<0.05, \*\*p<0.01, \*\*\*p<0.001 vs. vehicle; ###p<0.001 vs. 30  $\mu$ M. AzureSpot analysis software. Each density was normalized as compared to b-actin, and data are presented as the mean ± SD.

Fig. 4. Dose-dependent effects of FK-506 in NRK-52E and NRK-49F cells.

Fibrogenic responses of cocultured NRK-52E cells focusing on fibrosis. Following 2 days after 10 µM FK-506 treatment, NRK-49F cells  $(96.29 \pm 7.85 \%; p=0.052)$ decreased cell viability as compared to NRK-52E cells (103.59  $\pm$  2.47 %). Co-cultured NRK-52E cells showed cell viability of  $94.80 \pm 3.14$ % (p=0.000 vs. vehicle; p<0.001 vs. culture). Following consecutive 2 days after 30 µM FK-506 treatment, NRK-49F cells  $(76.12 \pm 12.38 \%; p=0.092)$ decreased cell viability as compared to NRK-52E cells (83.43  $\pm$  4.83 %). Co-cultured NRK-52E cells showed cell viability of  $76.60 \pm 4.34 \%$ (p<0.001 vs. vehicle; p=0.003 vs. single culture). (Fig. 5A)

αSMA immunostaining showed stronger in NRK-52E cells after 10 µM FK-506 treatment, but slightly weaker after consecutive 30 µM FK-506 treatment (Fig. 5B).

When NRK-52E cells were co-cultured with NRK-49F cells, the changes on fibrosis markers were investigated after FK-506 treatment by Western blotting (Fig. 5C). Fibronectin increased in co-cultured condition at 2 days (p=0.000), but not at 4 days (p=0.061). Fibronectin showed 1.81  $\pm$  0.46 fold (p=0.002 vs. vehicle, p=0.002 vs. FK-506 10 µM) in co-cultured NRK-52E cells at 2 days. Vimentin increased in cocultured condition at 2 days (p<0.001) and 4 days (p=0.039). Vimentin increased  $1.09 \pm 0.07$  fold (p=0.002 vs. vehicle) and  $1.35 \pm 0.22$ fold (p=0.000 vs. vehicle; p=0.001 vs. FK-506 10 µM) at 2 days, and  $1.11 \pm 0.15$  fold (p=0.081) and 1.31  $\pm$  0.40 fold (p=0.018 vs. vehicle, p=0.073 vs. FK-506 10 µM) at 4 days. αSMA expression was decreased in co-cultured condition at 2 days (p=0.010) and 4 days (p=0.002).  $\alpha$ SMA transiently increased at 10  $\mu$ M FK-506 (1.28  $\pm$ 



C. Cells were mock-treated with dimethyl sulfoxide (0) or treated with indicated dose of FK-506 for 2 days (Day 2) and subsequent 2 days (Day 4). Cells were harvested and whole cell extracts were subjected to immunoblotting using the indicated antibodies. Signal intensities of fibronectin, vimentin, αSMA, PARPI, LC3, GPX4, p27, and b-actin were A. NRK-49F, NRK-52E, and co-cultured NRK-52 cells were cultured in transwell mock-treated with dimethyl sulfoxide (0) or treated with 10 µM of FK-506 for 2 days, and subsequent 2 days with 30 µM of FK-506. The extent of cell viability was determined by MTT assay as described in Methods. Data are presented as mean ± SD. \*\*p<0.01, measured by AzureSpot analysis software. Each density was normalized as compared to b-actin, and data are presented as the mean ± SD. \*p<0.05, \*\*p<0.01, \*\*\*p<0.01 vs. B. NRK-52 cells were immunostained with αSMA antibody at different conditions as described in Methods. \*\*\* $p<0.001 \ vs.$  vehicle; ##p<0.01, ## $p<0.001 \ vs.$  NRK-52E with FK-506. vehicle; #p<0.05, ##p<0.01, ###p<0.001 vs. co-culture.

0.17 fold, p=0.010 vs. vehicle) at 2 days, but not observed in co-culture condition (0.89  $\pm$  0.31 fold, p=0.200 vs. vehicle, p=0.001 vs. single culture) at 2 days and any condition at 4 days with 30  $\mu$ M FK-506.

The cell death-related markers at 2 and 4 days, such as PARP1 (p=0.169 and p=0.600), LC3 (p=0.535 and p=0.025), and GPX4 (p=0.000 and p=0.210), were not significantly affected by FK-506 treatment in co-culture condition. P27 was significantly increased in co-cultured NRK-52E cells at 2 days (p=0.018), but not at 4 days

(p=0.152). P27 increased up to  $1.51 \pm 0.15$  fold (p=0.010 vs. vehicle, p=0.005 vs. single) at 2 days.

Selecting an appropriate cell line for renal fibrosis research. Respective kidney cell line shows characteristic expression for fibrosis markers (Fig. 6). Basal expression levels of fibrosis markers were compared among various kidney cell lines. Fibronectin was higher in HK-2 cell, vimentin was lower in TCMK and CRFK cells, and aSMA was lower in HK-2 and LLC-PK1 cells.

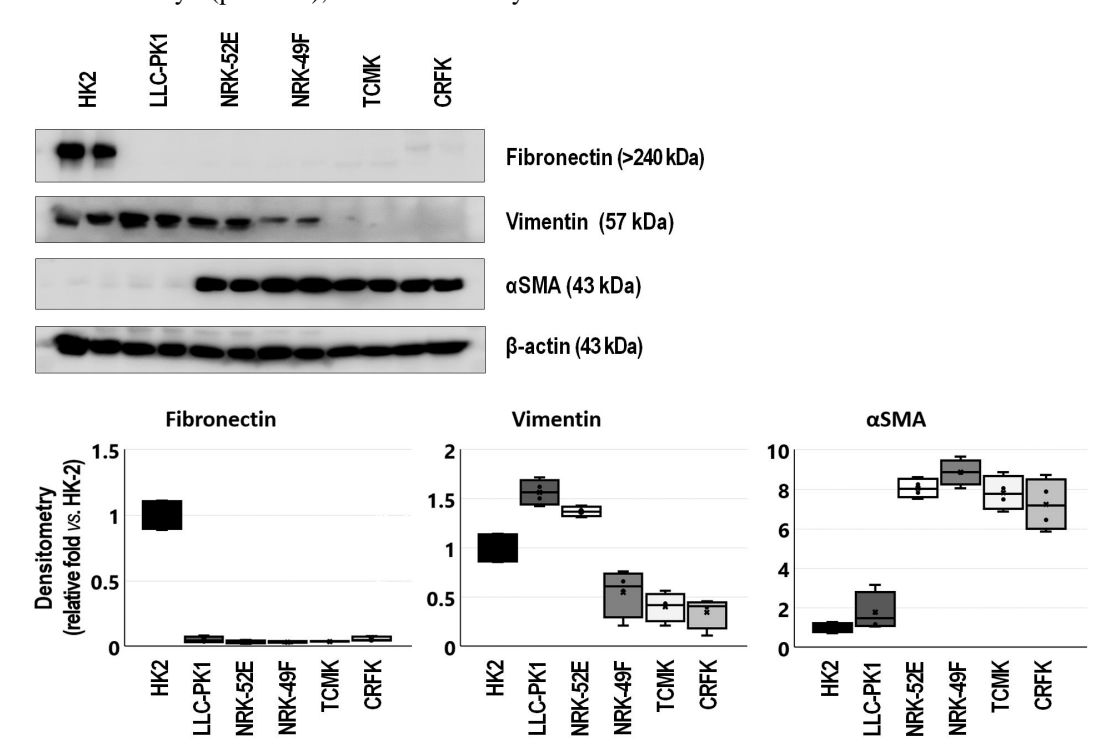


Fig. 6. Selecting an appropriate cell line for renal fibrosis research. Cells were cultured in conventional 2-dimensional environment for 2 days. Cells were harvested and whole cell extracts were subjected to immunoblotting using the indicated antibodies. Signal intensities of fibronectin, vimentin, aSMA, and b-actin were measured by AzureSpot analysis software. Each density was normalized as compared to b-actin, and data are presented as the mean  $\pm$  SD.

## DISCUSSION

FK-506 remains a cornerstone in immunosuppressive regimens for renal transplantation (Starzl *et al.*, 1990), yet its nephrotoxic effects, particularly tubulointerstitial fibrosis, can compromise long-term graft function (Olyaei *et al.*, 1999; Eberhardt *et al.*, 2018). In addition to FK-506-induced nephrotoxicity, TGF-β-induced EMT of NRK-52E cells and activation or myofibroblast transformation of NRK-49F cells are considered as underlying mechanisms of renal fibrosis induced by ureteral obstruction (Zhou *et al.*, 2021a), nephrectomy (Chang *et al.*, 2012), and lupus nephritis (Ijima *et al.*, 2022). Therefore, the respective characteristics were

assessed after FK-506 treatment. Our results demonstrate that low-dose FK-506, even below cytotoxic thresholds, can induce fibrogenic responses in both renal tubular epithelial cells and fibroblasts.

First of all, the cell type-specific characteristics were confirmed. While both cell types showed similar proliferation curves, NRK-49F cells showed more sensitivity to FK-506 than NRK-52E cells. NRK-52E cells showed higher N-cadherin and lower E-cadherin expression in accordance with the previous qualitative reports (Prozialeck *et al.*, 2003, 2004;

Nürnberger et al., 2010; Keller et al., 2012). Among fibrosis markers, NRK-52E cells showed higher vimentin expression than NRK-49F cells. EMT-like phenotype as appeared in spheroidogenesis was affected as conventional 2D culture. NRK-49F spheroids showed more sensitivity to FK-506 treatment than NRK-52E spheroids. The spheroids did not grow as time goes by, which means these cell lines might not be proper to spheroid cultures. As compared to 2D culture conditions, both spheroids showed lower N-cadherin, Ecadherin, and aSMA expression, but higher fibronectin and vimentin expression. Therefore, a careful concern on the previous fibrotic alteration with increased N-cadherin in NRK-49F cells and decreased E-cadherin in NRK-52E cells (Schulz et al., 2019) might be needed. Taken together, NRK-52E and NRK-49F cells represent the renal tubular epithelial cells and interstitial fibroblast cells, respectively. Unlike the marker of fibrosis of αSMA, spheroidogenesis with the decreased aSMA might not be an appropriate method for fibrosis research although it is believed to be mediated through EMT.

Secondly, dose-dependent cell death or cycle responses after FK-506 treatment (up to 30  $\mu$ M, not IC<sub>50</sub>) were checked. Apoptosis (PARP1) showed an increased tendency in NRK-49F cells after FK-506 treatment, but not in NRK-52E cells. Autophagy (LC3-II/I), ferroptosis (GPX4), and cell cycle arrest (p27) responses were not significantly changed in both cell lines. FK-506 treatment did not affect cell death responses in any culture condition, but cell cycle was transiently arrested by increased p27 expression in co-cultured NRK-52E cells. FK-506-induced apoptosis is well known in previous reports (Zheng et al., 2021; Cao et al., 2023; Nady et al., 2024), but autophagy remains controversial (Zheng et al., 2021; Cao et al., 2023). Nevertheless, there is controversy on the apoptosis of NRK-52E cell or renal epithelial cells. Zhang et al. (2019) reported that obstructive nephropathy-induced apoptosis of NRK-52E cells could aggravate renal interstitial fibrosis, but Ardura et al. (2008) suggested that increased fibronectin and aSMA in NRK-52E cells were observed in lower apoptotic tubulointerstitial cells in obstructive kidney. In addition, supernatant from human embryonic kidney 293 (HEK293) cells when mimicked like obstructive kidney could contribute to the inhibition of DNA synthesis in the NRK-49F cells (Nakamura et al., 2007). This study revealed that adequate dose of FK-506 could induce apoptosis but has little effect on autophagy, ferroptosis, and cell cycle. Therefore, lowdose FK-506 might be more appropriate for the fibrogenic researches.

Thirdly, dose-dependent fibrogenic responses after FK-506 treatment were checked. Vimentin increased in a dose-dependent manner in both cell lines, while fibronectin

did not show any considerable changes. Interestingly, αSMA transiently increased in 10 µM FK-506 but normalized or decreased in 30 μM FK-506. The transient increase of αSMA was further confirmed in a co-culture environment. When co-cultured with NRK-49F cells, NRK-52E cells showed a significant change in cell viability compared to the respective single culture. αSMA and fibronectin was transiently increased, while vimentin increased in a time-dependent manner in NRK-52E cells. When co-cultured with NRK-49F cells, extracellular acidosis (Schulz et al., 2022, 2023) decreased fibrosis and showed cytoprotective effects though nuclear factor erythroid 2-related factor 2 (Nrf2) and transketolase activation in NRK-52E cells. Thymocytes have promoting effects on the EMT of NRK-52E cells by downregulating E-cadherin and upregulating  $\alpha$ SMA and vimentin (Sun et al., 2025). Taken together, low dose FK-506 might induce fibrosis in both cell lines based on αSMA expression. But other fibrosis markers including fibronectin and vimentin responded differently, which means complex mechanisms in fibrosis need to be further investigated.

Lastly, the basal levels of fibrosis markers in various renal cell lines were investigated to provide an appropriate cell line for further renal fibrosis researches. Basal level of fibronectin was higher only in HK2 cells, vimentin lower in NRK-49F, TCMK, and CRFK cells, and αSMA lower in HK2 and LLC-PK1 cells. Therefore, appropriate cell lines should be adopted for the purpose of renal tubulointerstitial fibrosis research in terms of fibrosis markers. However, there are still extrinsic factors to consider when design the renal fibrosis researches. Hypoxia (Yang et al., 2021; Zhou et al., 2021b)- or obstruction (Zhao et al., 2021)-induced secretions including exosomes from NRK-52E cells could aggravate renal fibrosis by activating NRK-49F cells. Furthermore, acidosis led to an increase in vimentin in both cell lines, whereas co-culture, the effect was abolished. While acidosis led to an increased secretion of fibronectin in NRK-52E cells. not in NRK-49F cells, fibronectin secretion was decreased in co-culture (Schulz et al., 2022). These findings emphasize the need for early fibrosis biomarkers and support the development of combination anti-fibrotic strategies.

To overcome its nephrotoxicity, therapeutic drug monitoring is performed and suggested target ranges of 5-15 ng/mL of FK-506 in kidney transplant recipients (Marquet, 2025), which is comparable to  $0.006-0.018\,\mu\text{M}$  in *in vitro* experiment condition. As the *in vitro* study might be usually performed based on IC<sub>50</sub> including this study, relatively higher concentration might be adopted as compared to the clinical situation. Therefore, long-term treatment with lower concentration of FK-506 would be more compatible to overcome the clinical unmet needs, the FK-506-induced tubulointerstitial fibrosis.

In conclusion, our findings suggest that FK-506 contribute to early-stage tubulointerstitial fibrosis through epithelial-stromal interactions, even in the absence of overt cell death. These insights provide a foundation for future studies aimed at identifying early biomarkers of FK-506-induced nephrotoxicity and developing targeted anti-fibrotic strategies in the context of kidney transplantation and chronic immunosuppressive therapy.

**YOON, Y. KIM, H. L.; SHIN, B. C. & YOON, S. P.** FK-506 en dosis bajas contribuye a la fibrosis tubulointersticial mediante interacciones epiteliales-estromales. *Int. J. Morphol.*, *43*(*5*):1662-1673, 2025.

RESUMEN: El FK-506 es un fármaco inmunosupresor ampliamente utilizado para el trasplante renal, sin embargo presenta un efecto secundario común: la fibrosis tubulointersticial progresiva. Si bien se ha prestado atención a los fibroblastos por su papel en la fibrogénesis, aún queda por investigar el papel de las células epiteliales renales. Por lo tanto, nuestro objetivo fue evaluar las respuestas de las células epiteliales renales en comparación con los fibroblastos intersticiales renales tras el tratamiento con FK-506 para la fibrogénesis. Se obtuvieron células del túbulo proximal renal (NRK-52E) y células de fibroblastos intersticiales (NRK-49F) aisladas de ratas para la fibrogénesis renal inducida por FK-506. Las respuestas después del tratamiento con FK-506 se evaluaron mediante ensayo de viabilidad celular, esferoidogénesis, Western blotting e inmunocitoquímica. Las células NRK-52E mostraron mayor N-cadherina, mientras que las células NRK-49F mostraron mayor E-cadherina, fibronectina y actina de músculo liso alfa (αSMA). En comparación con las células NRK-52E, las células NRK-49F mostraron mayor sensibilidad a FK-506 por viabilidad celular y esferoidogénesis. La esferoidogénesis fue inducida por el aumento de fibronectina y vimentina en ambas células, mientras que las moléculas de adhesión celular, así como αSMA, disminuyeron. Las células NRK-49F, más sensibles, mostraron una tendencia al aumento de la apoptosis tras el tratamiento con FK-506, pero la autofagia, la ferroptosis y el ciclo celular no afectaron ninguna de las líneas celulares. El FK-506 a dosis bajas aumentó transitoriamente la expresión de αSMA en las células NRK-52E, lo que también se confirmó mediante el cocultivo de células NRK-52E, acompañadas de fibronectina. En conjunto, las células NRK-52E mostraron respuestas fibróticas tras el tratamiento con FK-506 a dosis bajas, con un aumento de la expresión de αSMA y fibronectina, que desapareció tras el tratamiento con FK-506 a dosis altas. Dado que los marcadores de fibrogénesis se expresaron de forma diferencial en diversas líneas celulares renales, se recomienda realizar más investigaciones mediante un diseño experimental más detallado.

PALABRAS CLAVE: FK-506; Fibrosis; Célula del túbulo proximal; Marcador.

#### REFERENCES

- Ardura, J. A.; Berruguete, R.; Rámila, D.; Alvarez-Arroyo, M. V. & Esbrit, P. Parathyroid hormone-related protein interacts with vascular endothelial growth factor to promote fibrogenesis in the obstructed mouse kidney. Am. J. Physiol. Renal Physiol., 295(2):F415-25, 2008.
- Baba, I.; Egi, Y.; Utsumi, H.; Kakimoto, T. & Suzuki, K. Inhibitory effects of fasudil on renal interstitial fibrosis induced by unilateral ureteral obstruction. *Mol. Med. Rep.*, 12(6):8010-20, 2015.
- Cao, G.; Miao, H.; Wang, Y. N.; Chen, D. Q.; Wu, X. Q.; Chen, L.; Guo, Y.; Zou, L.; Vaziri, N. D.; Li, P.; et al. Intrarenal 1-methoxypyrene, an aryl hydrocarbon receptor agonist, mediates progressive tubulointerstitial fibrosis in mice. Acta Pharmacol. Sin., 43(11):2929-45, 2022.
- Cao, R.; Li, Y.; Hu, X.; Qiu, Y.; Li, S.; Xie, Y.; Xu, C. L.; Lu, C.; Chen, G. & Yang, J. Glycyrrhizic acid improves tacrolimus-induced renal injury by regulating autophagy. FASEB J., 37(2):e22749, 2023.
- Chang, J. W.; Tsai, H. L.; Chen, C. W.; Yang, H. W.; Yang, A. H.; Yang, L. Y.; Wang, P. S.; Ng, Y. Y.; Lin, T. L. & Lee, O. K. Conditioned mesenchymal stem cells attenuate progression of chronic kidney disease through inhibition of epithelial-to-mesenchymal transition and immune modulation. J. Cell. Mol. Med., 16(12):2935-49, 2012.
- Chang, I.; Ohn, T.; Moon, D.; Maeng, Y. H.; Jang, B. G. & Yoon, S. P. SNU-333 cells as an appropriate cell line for the orthotopic renal cell carcinoma model. *Technol. Cancer Res. Treat.*, 20:15330338211038487, 2021.
- Chang, I. Y. & Yoon, S. P. Increased soluble E-cadherin of spheroid formation supplemented with fetal bovine serum in colorectal cancer cells. *Oncol. Lett.*, 25(5):207, 2023.
- Chen, H.; Yang, T.; Wang, M. C.; Chen, D. Q.; Yang, Y. & Zhao, Y. Y. Novel RAS inhibitor 25-O-methylalisol F attenuates epithelial-to-mesenchymal transition and tubulointerstitial fibrosis by selectively inhibiting TGF-βmediated Smad3 phosphorylation. *Phytomedicine*, 42:207-18, 2018.
- Deng, S.; Jin, T.; Zhang, L.; Bu, H. & Zhang, P. Mechanism of tacrolimusinduced chronic renal fibrosis following transplantation is regulated by ox-LDL and its receptor, LOX-1. Mol. Med. Rep., 14(5):4124-34, 2016.
- Eberhardt, W.; Nasrullah, U. & Pfeilschifter, J. Activation of renal profibrotic TGFb controlled signaling cascades by calcineurin and mTOR inhibitors. *Cell Signal.*, 52:1-11, 2018.
- Finn, W. F. FK506 nephrotoxicity. Ren. Fail., 21(3-4):319-29, 1999.
- Hira, K.; Sharma, P.; Mahale, A.; Prakash Kulkarni, O. & Sajeli Begum, A. Cyclo(Val-Pro) and Cyclo(Leu-Hydroxy-Pro) from *Pseudomonas* sp. (ABS-36) alleviates acute and chronic renal injury under *in vitro* and *in vivo* models (ischemic reperfusion and unilateral ureter obstruction). *Int. Immunopharmacol.*, 103:108494, 2022.
- Huang, X. L.; Zhou, Y. T.; Yan, Y. M. & Cheng, Y. X. Sesquiterpenoid-chromone heterohybrids from agarwood of Aquilaria sinensis as potent specific Smad3 phosphorylation inhibitors. J. Org. Chem., 87(12):7643-8, 2022.
- Ijima, S.; Saito, Y.; Nagaoka, K.; Yamamoto, S.; Sato, T.; Miura, N.; Iwamoto, T.; Miyajima, M. & Chikenji, T. S. Fisetin reduces the senescent tubular epithelial cell burden and also inhibits proliferative fibroblasts in murine lupus nephritis. Front. Immunol., 13:960601, 2022.
- Keller, C.; Kroening, S.; Zuehlke, J.; Kunath, F.; Krueger, B. & Goppelt-Struebe, M. Distinct mesenchymal alterations in N-cadherin and E-cadherin positive primary renal epithelial cells. *PLoS One.*, 7(8):e43584, 2012
- Liang, L.; Huang, K.; Yuan, W.; Liu, L.; Zou, F. & Wang, G. Dysregulations of miR-503-5p and Wnt/b-catenin pathway coordinate in mediating cadmium-induced kidney fibrosis. *Ecotoxicol. Environ. Saf.*, 224:112667, 2021
- Marquet, P. Getting tacrolimus dosing right. *Ther. Drug Monit.*, 47(1):41-8, 2025.
- Nady, M. E.; El-Raouf, O. M. A. & El-Sayed, E. M. Linagliptin ameliorates tacrolimus-induced renal injury: role of Nrf2/HO-1 and HIF-1α/CTGF/ PAI-1. Mol. Biol. Rep., 51(1):608, 2024.
- Nakamura, A.; Sakai, Y.; Ohata, C. & Komurasaki, T. Expression and significance of a disintegrin and metalloproteinase with thrombospondin motifs (ADAMTS)-1 in an animal model of renal interstitial fibrosis induced by unilateral ureteral obstruction. *Exp. Toxicol. Pathol.*, 59(1):1-7, 2007.

- Nürnberger, J.; Feldkamp, T.; Kavapurackal, R.; Opazo Saez, A.; Becker, J.; Hörbelt, M. & Kribben, A. N-cadherin is depleted from proximal tubules in experimental and human acute kidney injury. *Histochem. Cell Biol.*, 133(6):641-9, 2010.
- Olyaei, A. J.; de Mattos, A. M. & Bennett, W. M. Immunosuppressant-induced nephropathy: pathophysiology, incidence and management. *Drug Saf.*, 21(6):471-88, 1999.
- Prozialeck, W. C.; Lamar, P. C. & Lynch, S. M. Cadmium alters the localization of N-cadherin, E-cadherin, and beta-catenin in the proximal tubule epithelium. Toxicol. Appl. Pharmacol., 189(3):180-95, 2003. Erratum in: Toxicol. Appl. Pharmacol., 193(3):394, 2003.
- Prozialeck, W. C.; Lamar, P. C. & Appelt, D. M. Differential expression of Ecadherin, N-cadherin and beta-catenin in proximal and distal segments of the rat nephron. *BMC Physiol.*, 4:10, 2004.
- Ruiz-Ortega, M.; Bustos, C.; Plaza, J. J. & Egido, J. Overexpression of extracellular matrix proteins in renal tubulointerstitial cells by plateletactivating-factor stimulation. *Nephrol. Dial. Transplant.*, 13(4):886-92, 1998.
- Sakairi, T.; Hiromura, K.; Takahashi, S.; Hamatani, H.; Takeuchi, S.; Tomioka, M.; Maeshima, A.; Kuroiwa, T. & Nojima, Y. Effects of proteasome inhibitors on rat renal fibrosis in vitro and in vivo. Nephrology (Carlton), 16(1):76-86, 2011.
- Sasaki, K.; Doi, S.; Nakashima, A.; Irifuku, T.; Yamada, K.; Kokoroishi, K.; Ueno, T.; Doi, T.; Hida, E.; Arihiro, K.; Kohno, N. & Masaki, T. Inhibition of SET domain-containing lysine methyltransferase 7/9 ameliorates renal fibrosis. J. Am. Soc. Nephrol., 27(1):203-15, 2016.
- Schulz, M. C.; Gekle, M. & Schwerdt, G. Epithelial-fibroblast cross talk aggravates the impact of the nephrotoxin ochratoxin A. Biochim. Biophys. Acta Mol. Cell. Res., 1866(12):118528, 2019.
- Schulz, M. C.; Voß, L.; Schwerdt, G. & Gekle, M. Epithelial-fibroblast crosstalk protects against acidosis-induced inflammatory and fibrotic alterations. *Biomedicines*, 10(3):681, 2022.
- Schulz, M. C.; Dubourg, V.; Nolze, A.; Kopf, M.; Schwerdt, G. & Gekle, M. Acidosis activates the Nrf2 pathway in renal proximal tubule-derived cells through a crosstalk with renal fibroblasts. *Antioxidants (Basel)*, 12(2):412, 2023.
- Shigematsu, T.; Tajima, S.; Fu, R.; Zhang, M.; Itoyama, Y.; Tsuchimoto, A.; Egashira, N. & Ieiri, I. The mTOR inhibitor everolimus attenuates tacrolimus-induced renal interstitial fibrosis in rats. *Life Sci.*, 288:120150, 2022
- Starzl, T. E.; Fung, J.; Jordan, M.; Shapiro, R.; Tzakis, A.; McCauley, J.; Johnston, J.; Iwaki, Y.; Jain, A.; Alessiani, M.; et al. Kidney transplantation under FK 506. JAMA, 264(1):63-7, 1990.
- Sun, H.; Wang, X.; Liu, Y.; Yu, S.; Yang, Y.; Wu, S. & Zhang, C. Thymocytes induce renal tubular epithelial cells to undergo the epithelial-tomesenchymal transition. *Asian Pac. J. Allergy Immunol.*, 43(1):111-23, 2025.
- Wang, M.; Wang, L.; Zhou, L.; Xu, Y. & Wang, C. Shen-Shuai-II-Recipe inhibits tubular inflammation by PPARa-mediated fatty acid oxidation to attenuate fibroblast activation in fibrotic kidneys. *Phytomedicine*, 126:155450, 2024a.
- Wang, M.; Wang, J.; Wang, L.; Feng, X.; Qian, Y.; Ye, C. & Wang, C. Icariside II prevents kidney fibrosis development in chronic kidney disease by promoting fatty acid oxidation. *Phytother. Res.*, 38(2):839-55, 2024b.
- Wen, J.; Ma, Z.; Livingston, M. J.; Zhang, W.; Yuan, Y.; Guo, C.; Liu, Y.; Fu, P. & Dong, Z. Decreased secretion and profibrotic activity of tubular exosomes in diabetic kidney disease. Am. J. Physiol. Renal Physiol., 319(4):F664-73, 2020.
- Yang, T.; Zhang, B.; Pat, B. K.; Wei, M. Q. & Gobe, G. C. Lentiviral-mediated RNA interference against TGF-beta receptor type II in renal epithelial and fibroblast cell populations *in vitro* demonstrates regulated renal fibrogenesis that is more efficient than a nonlentiviral vector. *J. Biomed. Biotechnol.*, 2010:859240, 2010.
- Yang, L.; Wang, M.; Zhou, Y.; Yang, J.; Ye, C. & Wang, C. Shen Shuai II recipe attenuates renal interstitial fibrosis by improving hypoxia via the IL-1b/c-Myc pathway. Evid. Based Complement. Alternat. Med., 2021:5539584, 2021.

- Yano, R.; Golbar, H. M.; Izawa, T.; Sawamoto, O.; Kuwamura, M. & Yamate, J. Participation of bone morphogenetic protein (BMP)-6 and osteopontin in cisplatin (CDDP)-induced rat renal fibrosis. *Exp. Toxicol. Pathol.*, 67(2):99-107, 2015.
- Yoon, S. P. Orostachys japonica induces ferroptosis in 5-fluorouracilresistance acquired SNU-C5 colorectal cancer cells. Int. J. Morphol., 42(6):1508-16, 2024.
- Yu, J. B.; Lee, D. S.; Padanilam, B. J. & Kim, J. Repeated administration of cisplatin transforms kidney fibroblasts through G2/M arrest and cellular senescence. *Cells*, 11(21):3472, 2022.
- Yu, J. B.; Padanilam, B. J. & Kim, J. Activation of Yes-associated protein is indispensable for transformation of kidney fibroblasts into myofibroblasts during repeated administration of cisplatin. Cells, 13(17):1475, 2024.
- Zhang, X. F.; Yang, Y.; Zhang, J. & Cao, W. Microvesicle-containing miRNA-153-3p induces the apoptosis of proximal tubular epithelial cells and participates in renal interstitial fibrosis. *Eur. Rev. Med. Pharmacol. Sci.*, 23(22):10065-71, 2019.
- Zhao, S.; Li, W.; Yu, W.; Rao, T.; Li, H.; Ruan, Y.; Yuan, R.; Li, C.; Ning, J.; Li, S.; et al. Exosomal miR-21 from tubular cells contributes to renal fibrosis by activating fibroblasts via targeting PTEN in obstructed kidneys. *Theranostics*, 11(18):8660-73, 2021.
- Zheng, H. L.; Zhang, H. Y.; Zhu, C. L.; Li, H. Y.; Cui, S.; Jin, J.; Piao, S. G.; Jiang, Y. J.; Xuan, M. Y.; Jin, J. Z.; et al. L-Carnitine protects against tacrolimus-induced renal injury by attenuating programmed cell death via PI3K/AKT/PTEN signaling. Acta Pharmacol. Sin., 42(1):77-87, 2021.
- Zheng, J. Y.; Wang, S. C.; Tang, S. C.; Hsin, I. L.; Kang, Y. T.; Hsu, C. T.; Ou, C. C. & Ko, J. L. Sodium acetate ameliorates cisplatin-induced kidney injury in vitro and in vivo. Chem. Biol. Interact., 369:110258, 2023.
- Zhou, R.; Liao, J.; Cai, D.; Tian, Q.; Huang, E.; Lü, T.; Chen, S. Y. & Xie, W. B. Nupr1 mediates renal fibrosis via activating fibroblast and promoting epithelial-mesenchymal transition. FASEB J., 35(3):e21381, 2021a.
- Zhou, X.; Zhao, S.; Li, W.; Ruan, Y.; Yuan, R.; Ning, J.; Jiang, K.; Xie, J.; Yao, X.; Li, H.; et al. Tubular cell-derived exosomal miR-150-5p contributes to renal fibrosis following unilateral ischemia-reperfusion injury by activating fibroblast in vitro and in vivo. Int. J. Biol. Sci., 17(14):4021-33, 2021b.

Corresponding author:
Byung Chul Shin, M.D., Ph.D
Department of Internal Medicine
Chosun University Hospital
Chosun University College of Medicine
365 Philmun-daero
Dong-gu
Gwangju 61452
REPUBLIC OF KOREA

E-mail: bcshin@chosun.ac.kr

Corresponding author:
Sang-Pil Yoon, M.D., Ph.D.
Department of Anatomy
College of Medicine
Jeju National University
102 Jejudaehak-ro
Jeju-Si
Jeju-Do 63243
REPUBLIC OF KOREA

E-mail: spyoon@jejunu.ac.kr